

Understanding the Mechanism of Uranium Removal from Groundwater by Zero-Valent Iron Using X-ray Photoelectron Spectroscopy

JOSEPH N. FIEDOR,^{†,‡}
WILLIAM D. BOSTICK,^{*,†}
ROBERT J. JARABEK,[†] AND
JAMES FARRELL[§]

Materials and Chemistry Laboratory, East Tennessee
Technology Park, P.O. Box 2003,
Oak Ridge, Tennessee 37831-5808, and Department of
Chemical and Environmental Engineering, University of
Arizona, Tucson, Arizona 85721-0011

The contaminant of most concern in groundwater at the Oak Ridge Y-12 Plant's Bear Creek Valley Characterization Area is soluble uranium. The removal mechanism of soluble uranium from groundwater by zero-valent iron (ZVI, Fe⁰) was investigated. X-ray photoelectron spectroscopy (XPS, ESCA) was used to determine the uranium oxidation state at the Fe⁰ or iron oxide surface. Product speciation and relative reaction kinetics for the removal of soluble uranium under aerobic and anaerobic conditions with ZVI are presented. Under aerobic conditions, U⁶⁺ is rapidly and strongly sorbed to hydrous ferric oxide particulates ("rust"), whereas U⁶⁺ is slowly and incompletely reduced to U⁴⁺ under anaerobic conditions.

Introduction

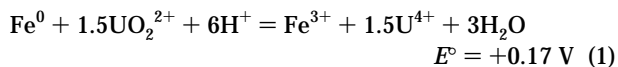
A concerted effort is under way to remediate groundwater contaminated with radionuclides (e.g., ⁹⁹Tc, U), other regulated metals (e.g., Hg²⁺, Cr⁶⁺), and volatile organic compounds (VOCs) at the Oak Ridge Y-12 Plant's Bear Creek Valley Characterization Area. Zero-valent iron (ZVI, Fe⁰) has been identified as a leading potential technology for use in this remediation effort. Previous works have demonstrated that ZVI can effectively remove Cr⁶⁺, Hg²⁺, Ag¹⁺, Tc⁷⁺, and U⁶⁺ from solution (1).

Soluble uranium (UO₂²⁺) is the contaminant of most concern in the Bear Creek Valley watershed. Soluble uranium is associated with both toxicity and cancer risks for the potential human receptors in the surrounding areas. Studies have shown that iron based minerals, such as pyrite or magnetite, can effectively adsorb U from groundwater under favorable conditions (i.e., E_h, pH, dissolved O₂, etc.). Recently, Cantrell et al. (2) were able to show that ZVI particles can be used to rapidly remove UO₂²⁺ (i.e., U⁶⁺) from a surrogate groundwater stream. They proposed that UO₂²⁺ may be removed from solution by any of three mechanisms: (a) reduction of U⁶⁺ by ZVI to form the less soluble U⁴⁺ (i.e., UO₂·xH₂O) phase, (b) sorption onto iron oxide corrosion

products by ion exchange with hydroxyl sites, or (c) a combination of reduction/precipitation. However, the mechanism by which ZVI facilitates the removal of U⁶⁺ from solution is still not well understood.

The goal of this study is to gain a better understanding of the mechanistic aspects (e.g., chemisorption, redox and/or coprecipitation) of U⁶⁺ removal by ZVI from a synthetic surrogate of Bear Creek Valley groundwater. Sorption, as a removal mechanism, is not preferred because soluble uranium will remain in its more soluble oxidation state (i.e., U⁶⁺), thereby lending itself to be easily transported by the colloidal iron corrosion products. Due to the reversible nature of the sorption mechanism, another concern is the potential release of soluble uranium back into the groundwater. Reduction of U⁶⁺ to U⁴⁺ is the preferred removal mechanism since the resulting U⁴⁺ species is less soluble and thus less mobile in groundwater, assuming that the U⁴⁺ species is not colloidal. Therefore, the solubility of uranium in groundwater plays an important role when considering effective strategies for its remediation.

Thermodynamically reduction to U⁴⁺ is *slightly* favorable in strongly acidic media as indicated by the modest positive value for the standard cell potential, E° in eq 1:



However, reports by Wersin et al. (3) indicate that reduction to the less soluble U⁴⁺ (e.g., UO₂·xH₂O) is controlled kinetically and not thermodynamically. Similarly, reduction of U⁶⁺ by the ferrous ion (Fe²⁺) has been reported to be kinetically slow except in the presence of strong acid (4).

It has been speculated that contaminants are removed by ZVI via a heterogeneous surface reaction (e.g., reduction, adsorption, and/or coprecipitation) that is able to render the contaminants insoluble and thus immobilize them onto the ZVI or iron oxide surface. It has also been long understood that the oxidation state of uranium is one of the determining factors that governs its solubility, speciation, and sorptive behavior (3). Therefore, any knowledge gained concerning the chemical speciation of uranium in solution and at the iron surface will provide valuable insight to the sorption/reduction processes.

X-ray photoelectron spectroscopy (XPS) is a surface-sensitive technique (i.e., analysis depth ≈ 100 Å) whose strength lies in its ability to determine the various chemical states of a given surface species. Previous studies have shown that XPS can be a valuable spectroscopic tool when studying the metal sorption processes, such as redox reactions, on oxide, clay, and sulfide systems (5, 6). Recently, Muftikian et al. (7) used XPS to examine the bimetallic surface of a palladium–iron system in an attempt to understand the dechlorination of VOCs. Other analytical methods, such as wet chemistry, used to determine the quantitative speciation of uranium often underestimate the contribution from U⁴⁺ due to reoxidation (8). In this way, XPS offers a significant contribution in determining uranium speciation, and thus this technique will be used in this study to monitor the uranium oxidation state at the iron surface.

The experimental design used in this study will enable one to monitor the uranium speciation as well as the relative kinetics for the removal of soluble uranium (U⁶⁺) in a synthetic surrogate of Bear Creek Valley groundwater by ZVI under the two limiting conditions of aerobic (oxic) and anaerobic (anoxic) experienced in remediation schemes using ZVI. The uranium speciation in solution will be kept relatively constant

* To whom correspondence should be addressed; phone: (423)-574-6827; fax: (423)576-8558; e-mail: wdbostick@aol.com.

[†] East Tennessee Technology Park.

[‡] Present address: Bettis Atomic Power Laboratory, Westinghouse Electric Company, West Mifflin, PA 15222.

[§] University of Arizona.

TABLE 1. Formulation of Surrogate Water

compound	concentration (as formulated) (mg/L)	value reported in authentic BYBY (mg/L) ^a
MgSO ₄ ·7H ₂ O	Mg = 6.02; SO ₄ = 23.8	Mg = 5.1–8.5 {5.8} SO ₄ = 8–21 {23.5}
CaCl ₂ ·2H ₂ O	Ca (total) = 50; Cl = 19.8	Ca = 38–76 {51.7} Cl = 20–33 {12.6}
Ca(OH) ₂		
NaHCO ₃	Na = 12.3	Na = 13–18 {≤9}
K ₂ CO ₃ ·1.5H ₂ O	K = 7.2	K = 3.9–6.1 {5.4}
NO ₃ ⁻	NA	NO ₃ ⁻ = 0.06 {<1}
total alkalinity (as CaCO ₃ , mg/L)	132	81–238 {160}
pH ^b	[~6.0]	{6.8}

^a Range of values, as summarized in Bostick et al. (12). These samples were not filtered prior to analysis, and thus silt, etc., add to the values reported for Al, Si, and Fe. (Total suspended solids for this data set was 23–326 mg/L). Values in brackets ({}) are the median of values from two batches of filtered samples as reported in Table 2 of Bostick et al. ^b Simulant was prepared by adding the stated chemicals to deionized water; calcium ion was solubilized; and the final pH was adjusted by bubbling a gas mixture (80% N₂/20% CO₂) into slurry overnight. After the solution is stored for several days, excess CO₂ is lost, gradually raising the solution pH value to ~7.2 (authentic BYBY samples behave similarly).

by carrying out the experiments at constant pH (i.e., ~6.0) (9–11). These experiments will provide boundary conditions in that the aerobic experiment will thermodynamically favor the sorption mechanism of uranium to the Fe³⁺ corrosion products, while the anaerobic experiment will favor the reduction of U⁶⁺ to U⁴⁺. Redox potential (*E_h*), pH measurements, dissolved O₂ readings, and γ -counting of the solution will be taken to assist in determining the most thermodynamically stable uranium species and the most kinetically favored mechanism under the varying O₂ solution conditions.

Experimental Section

Composition of Surrogate. The groundwater investigated in this study is representative of that found near groundwater sampling well 087 (GW-087), which is located near the so-called boneyard/burnyard (BYBY) region of the Bear Creek Valley Characterization Area. The BYBY water contains relatively low levels of total dissolved solids (TDS), and the principal metal contaminant of potential concern is soluble uranium. Representative Bear Creek Valley water system data is summarized in Bostick et al. (12). For purposes of testing, a surrogate was formulated to reproduce the essential composition of BYBY groundwater (see Table 1).

The calcium in the surrogate, added predominantly as Ca(OH)₂, was solubilized by bubbling the solution overnight with a gas mixture containing 80% N₂/20%CO₂. The excess carbon dioxide converts the alkaline lime reagent into a soluble, buffered bicarbonate form (13). Soluble uranium, in the form of uranyl nitrate (UO₂(NO₃)₂·6H₂O), was added to test solutions either as natural abundant material or material enriched with γ -emitting isotope ²³³U. The final concentration of total uranium in the surrogate solutions was between 6 and 8 ppm.

Measurement of Solution Parameters. *pH.* Solution pH measurements were taken using an Orion model 920A pH/ISE meter and a Beckman combination electrode (39846). The pH electrode was calibrated using 4.00, 7.00, and 10.00 pH buffer solutions.

E_h. Redox potential (*E_h*) readings were taken of the BYBY surrogate water using an Orion model 701A digital ion analyzer and an Orion platinum-calomel combination electrode filled with Orion filling solution. The electrode was calibrated by rinsing it several times with distilled water

and placing it into a beaker of Light's solution. *E_h* measurements were obtained in the millivolt mode. Results were corrected to give equivalency to the standard hydrogen electrode (SHE). Pourbaix diagrams, which are representations of a chemical species thermodynamic predominance as a function of solution pH and *E_h*, were used to predict the predominant uranium species in solution under equilibrium conditions (14).

Dissolved O₂. Dissolved oxygen (Do) measurements expressed in ppm were taken using an Orion model 920A pH/ISE meter equipped with an Orion oxygen electrode (970899). Calibration was carried out according to the manufacturers procedure. Salinity was assumed to be <2 ppt.

γ -Counting. Solutions traced with γ -emitting ²³³U were counted on a Packard Auto-Gamma 500 instrument. A 2-mL aliquot aqueous filtered sample was taken as a function of time to measure the removal of soluble uranium. Filtered samples were obtained using a 0.20- μ m pore Millipore membrane media syringe. For both experimental conditions, filtered samples were also collected from a deionized water solution that was used to rinse the reacted iron coupon. For the aerobic experiment, the iron coupon was removed from solution, and the remaining solution was filtered using a 0.45- μ m pore silver filter. Material collected on the filter is representative of detached iron corrosion products. A filtered syringe sample was also taken from the filtrate.

X-ray Photoelectron Spectroscopy (XPS). XPS spectra were obtained using a PHI (Perkin-Elmer) 5000 series XPS spectrometer equipped with a dual anode (Al, *h* = 1486.6 eV and Mg, *h* = 1253 eV). For this experiment, the Al anode was utilized at a power of 400W (15 kV). The instrument was operated in the fixed analyzer transmission (FAT) mode with a pass energy of 17.9 eV for high-resolution scans. The analysis pressure was kept <1.0⁻⁷ Torr. The instrument was interfaced to a UNIX-based Apollo 3500 PC for data collection. All data analysis performed on the XPS spectra was carried out with help of Googly Software.

A series of stable U standards [e.g., uranyl nitrate(UO₂(NO₃)₂·6H₂O), UO₃, and UO₂] was collected to obtain reference peak positions and peak shapes for various U oxidation states (U⁶⁺ and U⁴⁺). Powdered samples, such as the standards, were ground and then applied as a thin layer onto double-sided sticky carbon tape. A standard iron coupon and the treated iron coupons were mounted onto the XPS sample holder using carbon double-sided sticky tape. To be consistent, binding energy values for all samples were referenced to the C 1s (284.5 eV) line.

U⁶⁺ surface species will slowly reduce when placed in a high vacuum and exposed to X-rays (15). Therefore, samples were analyzed for about 1 h to minimize reduction. Under these time conditions, no significant U peak shift was observed.

The Levenberg–Marquardt damping method (16) was used for curve fitting U 4f envelopes. All peaks were fitted using a Voigt function (17) with 20% Lorentzian character. The background was assumed to be integral, and it was applied individually to each peak. The U 4f_{5/2}/U 4f_{7/2} area ratio for the spin-orbit doublet was fixed at 0.75. The separation between the U 4f_{5/2} and U 4f_{7/2} was set at 10.9 eV and the width ratio was assumed to be unity.

Experimental Solution Conditions. Small ZVI coupons (~5/9 in. diameter by 1/16 in. thick) were punched from mild steel plate. X-ray fluorescence analysis indicated that the coupon contained trace impurities of Al and Si in the bulk phase. The surface of the coupon was “cleaned” by soaking it briefly (~15 min) in 6 M HCl. Following a deionized water rinse, an acetone rinse, and a brief air-drying, the coupon was quickly placed into solution. A 300-mL surrogate solution spiked with 6–8 ppm ²³³U was placed into a 1-L

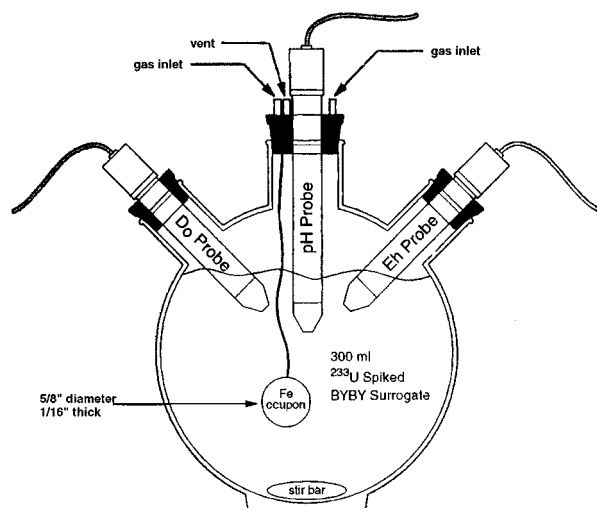


FIGURE 1. Experimental setup for the aerobic and anaerobic solution reactions. The anaerobic experiment was carried out in a radiological glovebox.

three-neck flask that was fitted with calibrated electrodes to monitor the solution's E_h , pH, and dissolved O_2 values. The ZVI coupon was suspended in solution by tying a piece of Kevlar string through a small hole that was drilled into the coupon. The experimental setup for both aerobic and anaerobic solutions is illustrated in Figure 1.

Aerobic. Aerobic solution conditions were maintained by purging the surrogate solution with O_2 . To sustain ~100% relative humidity, the purged gas streams were passed through a bubbler containing H_2O before entering into the surrogate. A constant pH (i.e., ~6.0) in the solution was obtained by concurrently purging with an 80% N_2 /20% CO_2 gas mixture. The CO_2 in the gas stream forms H_2CO_3 (i.e., bicarbonate) in solution that behaves like a buffer. With CO_2 bubbling in the solution, it is a concern that siderite (i.e., $FeCO_3$) can precipitate onto the surface of the iron coupon. In a laboratory test using a similar experimental design, it was estimated that the maximum iron substrate loss over 40 h due to aerobic corrosion would correspond to $\sim 3.6 \times 10^{-4}$ M. It should be noted and emphasized that under anaerobic conditions the corrosion and substrate loss will occur at a much slower rate. Therefore, assuming that $FeCO_3$ begins to precipitate when the Fe^{2+} concentration reaches 3×10^{-4} M, very little siderite formation is expected under our experimental conditions (18). Thus, in contrast to long-term operation of relatively high surface area particulate iron in a packed bed configuration (high solid surface/liquid volume), our geometry and experimental conditions for the relatively short-term coupon test (low solid surface/liquid volume) are not favorable to saturation and precipitation of siderite.

After 9.5 h in the aerobic U-traced solution, the iron coupon was removed. It was immediately rinsed with deionized water purged of CO_2 to remove any unbound corrosion products and placed on a planchet for subsequent XPS analysis. The remaining solution was filtered using a 0.45- μ m pore size filter from Millipore. The filtrate was sampled and analyzed for activity. The corrosion products remaining on the filter were scraped off and subsequently analyzed using XPS.

Anaerobic. Anaerobic conditions were maintained within a radiological glovebox using a continuous gas purge stream consisting of 80% N_2 /20% CO_2 . It was found that the pH of the solution rose over time if N_2 was used alone. The purge gas was first bubbled into a sealed scrubber tower containing water, to maintain ~100% relative humidity, and then passed into a radiological glovebox. The moistened purge gas was

TABLE 2. Final Conditions of the Iron Coupon Experiments

experiment	elapsed time (h)	final uranium concn (C/C_0)	final E_h /pH/ D_0
aerobic	10	0.78	+510 mV/5.8/17 ppm
anaerobic	72	0.45	-35 mV/6.0/0 ppm

then fed into a three-neck flask containing a test solution (see Figure 1). In a preliminary test lasting > 24 h using these experimental conditions, it was demonstrated that the gas purge maintained the test solution in the flask at a pH value near 5.7.

The glovebox was purged with the N_2 . This was done to ensure that the iron coupon would be exposed to a similar atmosphere when taken out of solution. The contents of the flask, with coupon, were purged with the N_2/CO_2 mixture for ~100 h. At this time, the iron coupon was removed, rinsed with deionized water purged of CO_2 to remove loosely bound soluble uranium, and placed into a sealable airtight sample holder to transport to the X-ray photoelectron spectrometer. In this manner, the reacted iron coupon would never be exposed to air.

Results and Discussion

Theoretical Thermodynamic Considerations. Assuming that the uranium species has reached equilibrium with the dominant Fe redox couple, the equilibrium speciation of soluble and adsorbed uranium can be predicted from the solution E_h and pH values for each experiment listed in Table 2. The solution conditions in the aerobic experiment favor $UO_3 \cdot 2H_2O$ as the most thermodynamically stable solid species and the uranyl ion (UO_2^{2+}) as the most stable aqueous species, as indicated by the Pourbaix diagram (E_h vs pH) for the uranium-water system considering UH_3 , U, UO , U_2O_3 , UO_2 , U_3O_8 , and $UO_3 \cdot 2H_2O$ (14). The Pourbaix diagram also indicates that U^{6+} should be reduced to U^{4+} at the potential of the Fe^0/Fe^{2+} redox couple, $E^0 = -0.44$ mV (14). Although the solution conditions predict U^{6+} as the stable uranium oxidation state, conditions at the zero-valent iron surface theoretically predict that reduction to U^{4+} is possible.

MINTEQA2 solution modeling of the aerobic coupon experiment also predicts that the dissolved uranium will be in the U^{6+} state in the form of complex ions with dissolved carbonate ion. The modeling indicates that the most predominant uranium containing species, $UO_2CO_3(aq)$, accounts for 67% of the total soluble uranium, while 32% of the uranium exists in decarbonate complexes as $UO_2(CO_3)_2^{2-}$.

The final solution E_h and pH values in the anaerobic experiment listed in Table 2 correspond to U^{4+} as the thermodynamically favored oxidation state. MINTEQA2 solution modeling also predicts U^{4+} as the predominant uranium species and indicates that at equilibrium more than 99% of the total uranium precipitates from solution as $UO_2 \cdot (c)$. However, because only 55% of the total uranium was removed from solution by the termination of the experiment, the modeling indicates that the dissolved uranium is not in equilibrium with the E_h of the bulk solution.

Spectroscopic Characterization. Standard Fe Coupon. The overall XPS spectrum for a freshly acid-washed iron coupon is illustrated in Figure 2A. The main elements on the coupon surface are iron, oxygen, and carbon. The overall XPS spectrum also indicates the presence of a small amount of chlorine, most likely a residue of the acid-washing procedure. An enlargement of the Fe 2p binding energy region from Figure 2A is shown in panel B. The Fe 2p spectrum indicates that iron oxide is the predominant surface species and that Fe^0 , as indicated by the arrow, is a minor component. The position of the Fe 2p_{3/2} peak at 710.8 eV is indicative of ferric iron, which may be present in any one

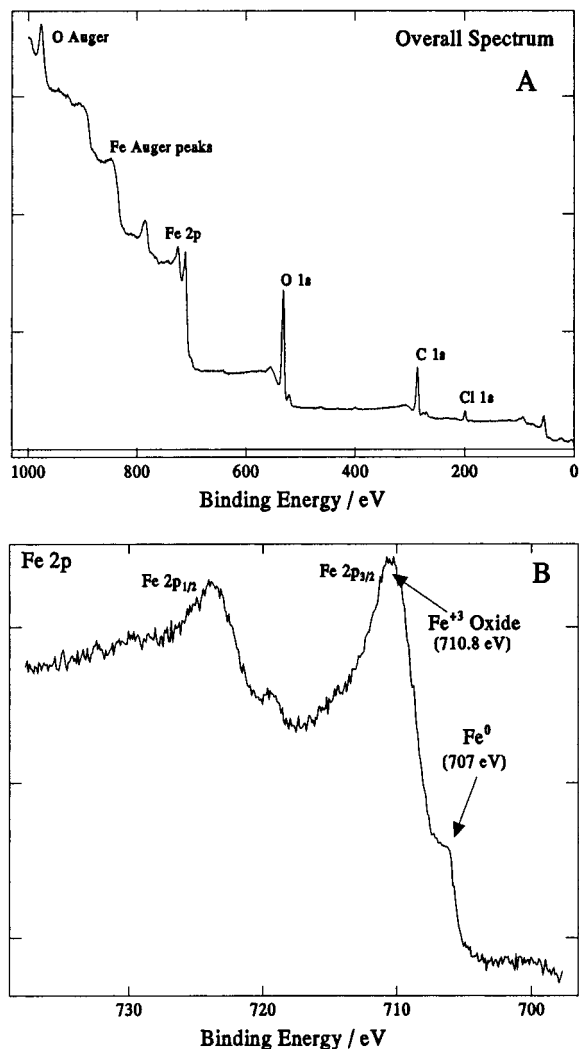


FIGURE 2. (A) Overall XPS spectrum of a freshly cleaned iron coupon. (B) Individual XPS Fe 2p binding energy region of the cleaned unreacted iron coupon.

of several possible species including hydrated ferric oxide (FeOOH), magnetite (Fe_3O_4), or hematite (Fe_2O_3). It is difficult for XPS to differentiate between these three Fe^{3+} containing species, but thermodynamic considerations would favor hydrated ferric oxide as the surface species (7). This analysis indicates that the iron surface reoxidizes rapidly, and thus any acid washing procedures must be performed under anaerobic conditions.

Aerobic: XPS—U Region. The U 4f spectra from the four samples obtained from the aerobic and anaerobic coupon experiments are plotted in Figure 3. The two lines indicate the U $4f_{7/2}$ peak positions corresponding to U^{6+} and U^{4+} oxidation states. The positions of the U^{6+} and U^{4+} species were determined from the spectra for three uranium standards: $\text{UO}_2(\text{NO}_3)_2 \cdot 6\text{H}_2\text{O}$, UO_3 , and UO_2 (see Figure 4). The standards indicate that the binding energy associated with the U $4f_{7/2}$ peak for U^{6+} occurs at 381.4 eV, while that for U^{4+} occurs at 379.8 eV. This binding energy difference of ~ 1.6 eV is in close agreement with previous studies (19, 20).

Figure 3C represents the U 4f spectrum for the iron coupon exposed to the surrogate solution under completely anaerobic conditions. It is evident that the U $4f_{7/2}$ peak position for this sample strongly correlates with the presence of a U^{4+} surface species. However, close examination of this envelope indicates that U^{4+} was not the only component present. Figure

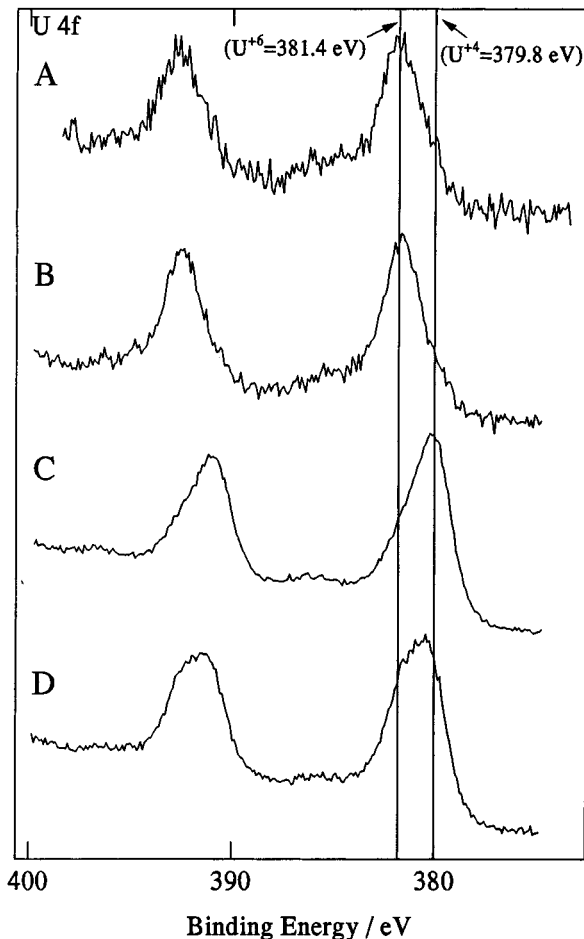


FIGURE 3. Overlay of the series of U 4f spectra generated from the aerobic and anaerobic experiments. (A) U 4f XPS spectrum of uranium sorped onto Fe^{3+} corrosion products formed during aerobic solution conditions. (B) U 4f XPS spectrum for iron coupon exposed to the surrogate solution under completely aerobic conditions. (C) U 4f XPS spectrum for iron coupon exposed to the surrogate solution under completely anaerobic conditions. (D) U 4f XPS spectrum for iron coupon exposed to lab air ($\sim 32\%$ relative humidity) for 2.7 h. The two lines indicate the U $4f_{7/2}$ peak positions of a U^{6+} species and a U^{4+} species.

3A shows a curve fitted spectrum of Figure 3C. The curve fitted U 4f envelope uses the individual peak areas to semiquantitatively estimate the contributions of U^{4+} and U^{6+} . Curve fitting variables for the individual uranium species, such as peak position (i.e., U $4f_{7/2}$ of $\text{U}^{6+} = 381.4$ eV and U $4f_{7/2}$ of $\text{U}^{4+} = 379.9$ eV), were approximated from the standards. Curve fitting results indicate that $\sim 75\%$ of the uranium adsorbed on the coupon surface is in the U^{4+} oxidation state, while $\sim 25\%$ is in the U^{6+} state. These results are consistent with the thermodynamic predictions based on the E_h/pH measurements, and they are very similar to those reported by Wersin et al. (3), who used similar techniques to demonstrate the partial reduction of U^{6+} by sulfide minerals under strongly reducing anaerobic conditions. Thus, even under extremely anaerobic conditions only partial reduction of U^{6+} is evident.

Next, the anaerobically reacted iron coupon was removed from the spectrometer and exposed to lab air ($\sim 32\%$ relative humidity) for 2.7 h and then reexamined by XPS (Figure 3D). This was done to determine the rate of reoxidation and thus gain an understanding of the crystal nature of the UO_2 species. It has been observed that moist amorphous $\text{UO}_2 \cdot 2\text{H}_2\text{O}$ will oxidize in air rather quickly to form $\text{UO}_3 \cdot \text{H}_2\text{O}$ (21). However, crystalline UO_2 hydrate is stable in air for several days at

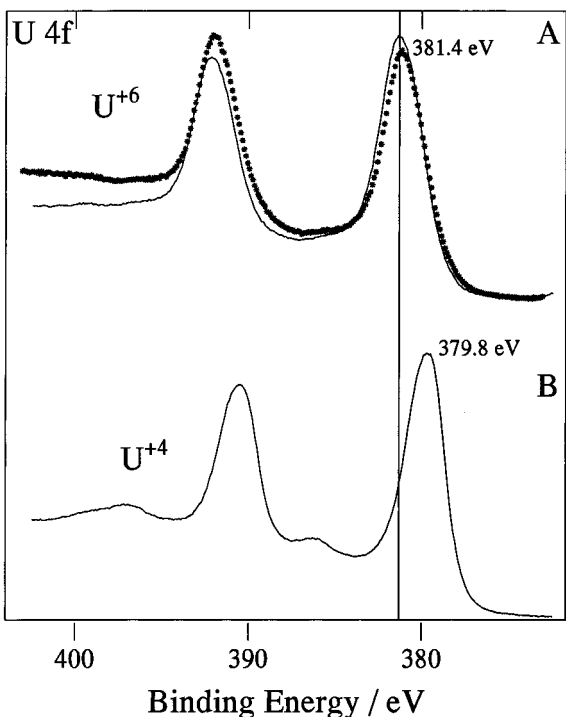


FIGURE 4. Overlay of the U 4f binding energy region for three uranium standards. The top spectrum overlays U⁶⁺ standards UO₂(NO₃)₂·6H₂O (—) and UO₃ (·). The bottom spectrum shows U⁴⁺ standard UO₂.

room temperature (21). Partial reoxidation of U⁴⁺ to U⁶⁺ was observed after short exposure to low-humidity air (see Figure 5B). It is estimated that ~25% of the U⁴⁺ reoxidized, resulting in an overall even distribution of U⁴⁺ and U⁶⁺. No further reoxidation occurred after ~16 h of additional exposure to air.

Aerobic: XPS—U Region. Figure 3B represents the U 4f envelope for the iron coupon that was reacted under aerobic conditions. The U 4f_{7/2} peak position of 381.6 eV corresponds to the presence of a U⁶⁺ surface species. Therefore, if appreciable oxygen is available, the predominant mechanism for the removal of soluble U⁶⁺ by iron is by sorption of U⁶⁺ to detached hydrolyzed Fe³⁺ corrosion product or to the iron oxide on the surface of the metal.

Aerobic/Anaerobic: XPS—Fe Region. Figure 6 overlays the Fe 2p spectra for the standard “clean” iron coupon, the anaerobically reacted iron coupon, and the aerobically reacted iron coupon. The Fe 2p spectrum of the anaerobically reacted iron coupon (Figure 6B) consists of only one iron component. This component has an Fe 2p_{3/2} binding energy of ~710.8 eV, which is indicative of an Fe³⁺ species. This is an interesting finding since anaerobic corrosion (see eq 2) should produce an abundance of Fe²⁺ species:



However, the presence of a thin surface layer of magnetite, which is a spinel structure that consists of octahedral sites occupied with approximately equal numbers of Fe²⁺ and Fe³⁺ atoms and tetrahedral sites occupied solely by Fe³⁺ atoms, cannot be ruled out (22). In fact, White et al. (22) showed that magnetite had an XPS Fe 2p_{3/2} peak position of 710.7 eV, which is indicative of an Fe³⁺ surface species and in agreement with our findings. Grambow et al. (8) gave further support by correlating the reduction of U⁶⁺ under anaerobic conditions to the presence of magnetite and attributed this to surface-mediated electron transfer at sorptive sites.

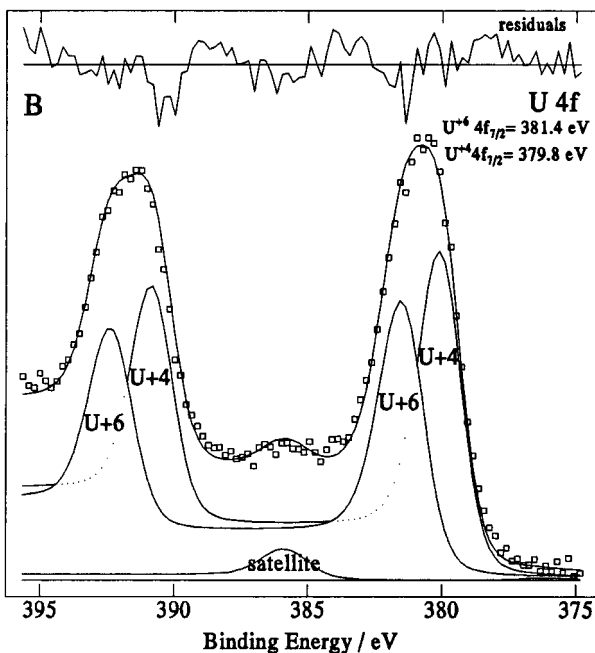
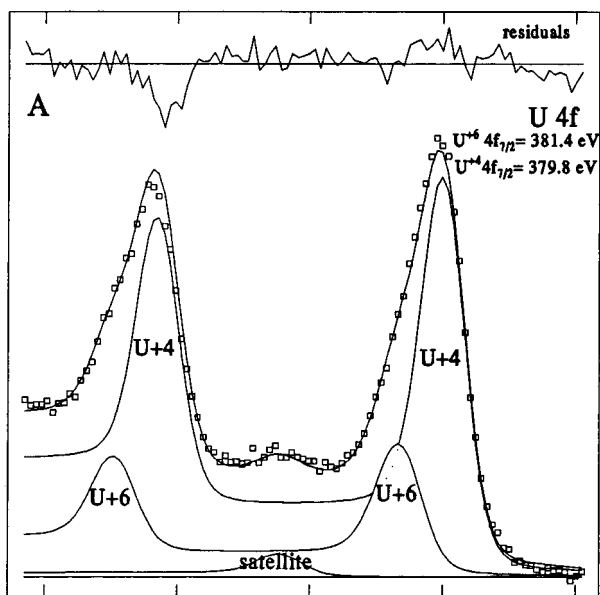


FIGURE 5. (A) Curve-fitted U 4f envelope of Figure 3C. (B) Curve-fitted U 4f XPS envelope of Figure 3D.

It can be postulated that the formation of a highly hydroxylated iron oxide film may facilitate the reduction of uranium. This hydroxylated layer may act as region where U⁶⁺ can actively adsorb to form U—O—Fe bonds. Upon adsorption in this manner, the uranium is immobilized long enough so that electrons may be donated to the U⁶⁺ surface species by the electron-rich iron oxide layer and/or the bulk Fe⁰. A similar mechanism has been proposed for the palladium—iron system (7).

Unlike the anaerobic experiment, the aerobic experiment produced copious amounts of Fe³⁺ corrosion products that sloughed off into solution. It appears that under aerobic conditions iron corrosion products are formed, loosely bound to the ZVI matrix and easily removed by a simple rinsing and/or agitation. To analyze the corrosion products for the sorption of uranium, the surrogate solution was filtered with a 0.45- μm silver filter from Millipore. Figure 6C represents the XPS Fe 2p region of the Fe corrosion products. The Fe 2p_{3/2} binding energy position of ~710.8 eV is suggestive of

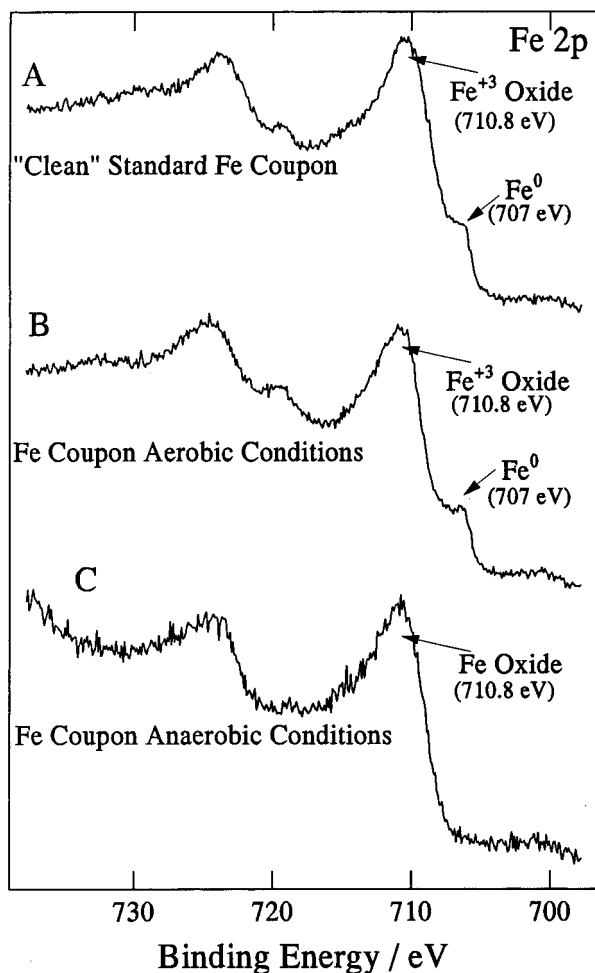


FIGURE 6. Overlay the Fe 2p spectra for the (A) standard "clean" iron coupon, (B) the anaerobically reacted iron coupon, and (C) the aerobically reacted iron coupon.

an Fe³⁺ surface species. Figure 3A shows the U 4f XPS spectrum for the Fe³⁺ corrosion products. The U 4f_{7/2} peak position of 381.6 eV indicates the presence of a U⁶⁺ surface species. Thus, sorption of U⁶⁺ to the highly hydrated Fe³⁺ most likely occurs via a proton exchange with the hydroxyl sites. Again, this finding is consistent with the thermodynamic predictions.

Figure 6B shows the Fe 2p XPS region of the iron coupon that was reacted aerobically. It is interesting to note that this Fe 2p spectrum is very similar in peak shape to that of the standard clean iron coupon (Figure 6A). In fact, both spectra show the presence of a surface Fe metal component and a thin layer of iron(III) oxide. A possible explanation of this phenomenon is that the formation and eventual removal of the iron(III) oxide layer due to aerobic corrosion enables the surface of the aerobic Fe coupon to be continuously replenished so that a clean surface is formed.

Kinetics. Figure 7 illustrates the relative kinetics for removal of soluble uranium under the limiting solution conditions of aerobic and anaerobic. The pseudo-first-order removal for the aerobic experiment (■) gave a half-life of ~9 h. Anaerobic testing (○) had notably slower relative kinetics for the removal of soluble uranium, with an apparent "induction" phase of >30 h, before yielding pseudo-first-order kinetics uranium removal kinetics with a half-life of ~63 h. Thus, removal of soluble U⁶⁺ by sorption occurs on the order of 7 times faster than the removal of soluble U⁶⁺ by reduction to the less soluble U⁴⁺. Grambow et al. (8) stated that at low uranium concentrations kinetic factors can slow the reduction reaction.

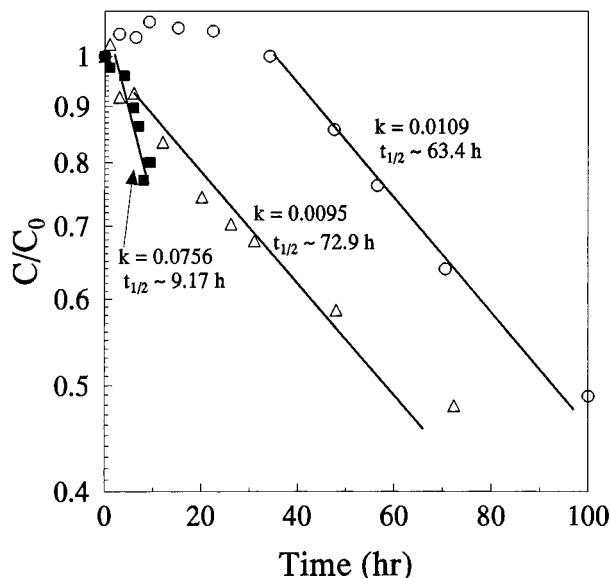


FIGURE 7. Relative kinetics for removal of soluble uranium under the limits of aerobic and anaerobic conditions: (■) iron coupon exposed to aerobic conditions, (○) iron coupon exposed to anaerobic conditions, (△) iron oxide coated iron coupon exposed to anaerobic conditions.

Presuming the reduction of U⁶⁺ is a surface-mediated effect, the lag period seen in the anaerobic experiment could be caused by the formation of sorptive sites. These sites could correlate with the growth of a thin highly porous layer of iron oxide due to anaerobic corrosion. To investigate this postulation, a ZVI coupon was exposed to an CO₂ atmosphere at 800 °C in attempt to prepare a thin layer of magnetite (Fe₃O₄) coating. Magnetite is geologically stable, has sorptive capabilities, and is conductive. These properties make it an ideal surface coating. However, X-ray diffraction (XRD) analysis indicated that both magnetite and hematite (Fe₂O₃) were present on the surface of the coupon in roughly equal proportions. The surface-coated coupon was exposed to the solution under anaerobic conditions in attempt to compare the kinetics with that of the ZVI coupons reacted under anaerobic and aerobic conditions. It is readily apparent from Figure 7 that the oxide-coated coupon (△) eliminates the lag phase, indicating that reduction is a surface-mediated effect. However, it does not accelerate the kinetics (t_{1/2} = ~72.9 h) for reduction of U⁶⁺ to U⁴⁺. XPS results for the iron oxide-coated ZVI coupon reacted under anaerobic conditions were analogous to the uncoated ZVI coupon (see Figure 3C) reacted under similar conditions. Thus, the thin layer of iron oxide did not hinder the partial reduction of U⁶⁺ species to U⁴⁺.

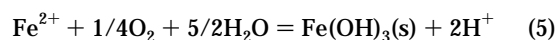
Discussions

Some of the more important reactions that may occur during treatment of metals (e.g., inorganics) with ZVI include the following processes:

anaerobic corrosion



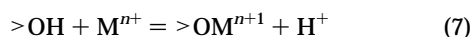
aerobic corrosion



cementation



sorption/ion exchange



For the aerobic experiment, eqs 4, 5, and 7 represent the most likely reaction mechanisms. The ZVI coupon is first oxidized in solution to form a ferrous iron (Fe^{2+}) layer. In turn, the ferrous iron (Fe^{2+}) is rapidly oxidized (eq 5) to form a high surface area and highly porous layer of hydrolyzed ferric (Fe^{3+}) oxide. Hydrolyzed ferric iron [$Fe(OH)_3(s)$] and its polymer, ferrihydrate, are effective in removing U^{6+} by sorption (depicted by eq 7) (23–27). In eq 7, the $>OH$ represents an exchangeable site on the hydrous metal oxide at the hydrous iron substrate or on its detached corrosion product. Note in the simplified eq 7 that, depending on the solution pH, the surface site may have a net positive charge ($>OH_2^+$) or negative ($>O^-$) charge. The exchange of protons to and from the oxide surface creates specific site types available for adsorption. For most iron-containing minerals, the solution pH value that results in no net charge on the mineral (i.e., the point of zero charge or pzc) is typically in the range of ~6–8 (28). As the solution pH falls below the pzc of the substrate, the net surface charge becomes more positive, favoring the sorption of anionic species; conversely, as the pH is increased above the pzc, the substrate becomes more negatively charged, favoring the sorption of cationic species. For our experiment, the iron surface contained roughly equal amounts of negative and positive charges because the pH (6.0) is close to the pzc of the iron substrate. Since both charges exist on the iron surface at this pH, sorption of U^{6+} by the iron surface can take place with the negatively charged $UO_2(CO_3)_2^{2-}$ species as is suggested by Payne and Waite (9) and further supported by the MINTEQA2 modeling performed in this experiment or the positively charged $(UO_2)_3(OH)_5^+$ species as predicted by Meinrath et al. (11).

For the anaerobic investigation, the “cementation” reaction seen in eq 5 ($M =$ uranium or UO_2^{2+}) most readily describes the mechanistic pathway by which soluble U^{6+} is removed from solution. Our work has shown that, under strongly reducing anaerobic conditions and given enough time, ZVI can partially reduce U^{6+} to U^{4+} . Our results are consistent with the literature for reduction of U^{6+} by Fe^{2+} or H_2 in that reduction of U^{6+} appears to be kinetically slow. Therefore, the relative significance of soluble uranium removal by reduction using ZVI under treatment trench conditions is uncertain.

Perhaps, with a deep enough treatment zone to provide the necessary anaerobic conditions and the required contact time, this mechanism could represent a significant component to the overall removal of soluble uranium, if any remains after the semi-oxic contact zone, which offers a relatively rapid removal of U^{6+} by sorption to corrosion product. Thus, if the residence time in a treatment trench is relatively short (e.g., less than a few hours) and anoxic conditions are not achieved fairly rapidly, then kinetically slow reduction of U^{6+} is not likely to be a significant component of the overall removal.

In the middle of a treatment trench, where anoxic conditions begin to prevail, the pH values will be considerably higher than pH 6 due to the production of hydroxyl ions from the relatively slow anaerobic corrosion of the iron substrate (eq 3). This is detrimental to the reduction mechanism because higher pH values (>8) tend to disfavor reduction of U^{6+} and favor sorption. Therefore, under practical groundwater remediation conditions, sorption

appears to have a more significant role than reduction in the removal of U^{6+} using ZVI. Most of the soluble uranium removal occurs under semi-oxic conditions near the forward portion of the column or trench, where U^{6+} can bind avidly to corrosion product containing Fe^{3+} . Thus, there will be little additional uranium removal downstream by reduction due to (a) unfavorable kinetics in the near-neutral to alkaline solution and (b) a low concentration of residual soluble U^{6+} available to be reduced.

In conclusion, iron coupons tested under controlled conditions indicate that under fully aerobic conditions sorption of U^{6+} to hydrated Fe^{3+} corrosion products is the predominant removal mechanism. The strong affinity for uranium by iron-containing minerals is well-documented (23–27). However, a potential concern with this removal mechanism is the possible redispersion and/or desorption of U^{6+} on detached fine particulate corrosion products. Although, treatment by ZVI of subsurface water, with low levels of dissolved oxygen, should minimize this effect.

When reaction conditions (pH and U speciation) are similar but with the exclusion of dissolved oxygen, soluble uranium is slowly removed at the iron surface by partial reduction of U^{6+} to a sparingly soluble U^{4+} species. Uranium speciation was verified using XPS. These results are similar to those reported by Grambow et al., who suggest that U^{6+} in anaerobic brine solution is sorbed to magnetite (Fe_3O_4) and then slowly and incompletely reduced at the iron surface (8). Analogously, Wersin et al. reported on the kinetically slow partial reduction of U^{6+} to U^{4+} at the surface of sulfide minerals under strongly reducing anoxic conditions (3). Therefore, reduction of uranium may be beneficial in terms of limiting its solubility and mobility, but the relatively slow reaction kinetics may mandate a long residence time in the reductive medium.

Acknowledgments

The authors would like to thank Richard Helferich of Cercona Inc. for the preparation of the ZVI coupon coated with iron oxide. We also thank Dr. Douglas Hoffmann of the Materials and Chemistry Laboratory for his valuable suggestions and critiques. Work was sponsored by the U.S. Department of Energy under Contract DE-AC05-84OR21400. This research was supported in part by an appointment to the Oak Ridge National Laboratory Postdoctoral Research Associates Program administered jointly by the Oak Ridge National Laboratory and the Oak Ridge Institute for Science and Education.

Literature Cited

- (1) For a complete list of references on this subject, please see WEB page maintained by Dr. Paul Tratnyek, www.ese.ogi.edu/ese.docs/tratnyek/ironrefs.html, Department of Environmental Science and Engineering, Oregon Graduate Institute of Science & Technology.
- (2) Cantrell, K. J.; Kaplan, D. I.; Wietsma, T. W. *J. Hazard. Mater.* **1995**, *42*, 201–212.
- (3) Wersin, P.; Hochella, M. F., Jr.; Persson, P.; Redden, G.; Leckie, J. O.; Harris, D. W. *Geochim. Cosmochim. Acta* **1994**, *58* (13), 2829–2843.
- (4) Baes, C. F., Jr. *The Reduction of Uranium (VI) by Ferrous Iron in Phosphoric Acid Solution: The Formal Electrode Potential of the U(IV)/U(VI) Couple*; Report ORNL-1581; Oak Ridge National Laboratory: Oak Ridge, TN, 1953.
- (5) Bancroft, G. M.; Hyland, M. M. *Rev. Mineral.* **1990**, *23*, 511.
- (6) Dillard, J. G.; Koppelman, M. H.; Crowther, D. L.; Schenk, C. V.; Murray, J. W.; Balisterieri, L. In *Adsorption From Aqueous Solution*; Tewari, P. H., Ed.; Plenum Press: New York, 1988; p 227.
- (7) Muftikan, R.; Nebesny, K.; Fernando, Q.; Korte, N. *Environ. Sci. Technol.* **1996**, *30*, 3593.
- (8) Grambow, B.; Smailos, E.; Geckis, H.; Mueller, R.; Hentschel, H. *Radiochim. Acta* **1996**, *74*, 149.
- (9) Payne, T. E.; Waite, T. D. *Radiochim. Acta* **1991**, *52/53*, 487.

- (10) Miyahara, K. *J. Nucl. Sci. Technol.* **1992**, 30, 314.
- (11) Meinrath, G.; Kato, Y.; Kimura, T.; Yoshida, Z. *Radiochim. Acta* **1996**, 75, 159.
- (12) Bostick, W. D.; Jarabek, R. J.; Slover, W. A.; Fiedor, J. N.; Farrell, J.; Helfferich, R. *Zero-Valent Iron and Metal Oxides for the Removal of Soluble Regulated Metals in Contaminated Groundwater at a DOE Site*; Report K/TSO-35P; Lockheed Martin Energy Systems, Inc.: Oak Ridge, TN, 1996.
- (13) Manahan, S. E. *Environmental Chemistry*, 6th ed.; Lewis Publishers: Boca Raton, 1994; pp 62–64.
- (14) Pourbaix, M. *Atlas of Electrochemical Equilibria in Aqueous Solutions*, 2nd English ed.; National Association of Corrosion Engineers: Houston, TX, 1974.
- (15) *Gmelin Handbook of Inorganic Chemistry: Uranium*, Vol. A5; Springer-Verlag: New York, 1982; p 185.
- (16) Press, W. H.; Flannery, B. P.; Teukolsky, S. A.; Vetterburg, W. T. *Numerical Recipes*; Cambridge University Press: Cambridge, MA, 1986.
- (17) Humlicek, J. J. *Quantum Spectrosc. Radiat. Trans.* **1979**, 21, 309.
- (18) Lange, N. A. *Handbook of Chemistry*, 10th ed.; McGraw-Hill Book Company, Inc.: New York, 1961.
- (19) Chadwick, D. *Chem. Phys. Lett.* **1973**, 21, 291.
- (20) Gorsuch, J. D.; Stewart, W. E. *Application of ESCA to The Analysis of Uranium Systems*; Report DP-MS-73-44; Savannah River Laboratory, E. I. du Pont de Nemours and Co.: Aiken, SC, 1973.
- (21) Katz, J. J.; Rabinowitz, E. *The Chemistry of Uranium: Part 1*; McGraw-Hill Publishers: New York, 1951.
- (22) White, A. F.; Peterson, M. L.; Hochella, M. F., Jr. *Geochim. Cosmochim. Acta* **1994**, 58 (8), 1859–1875.
- (23) Langmuir, D. *Geochim. Cosmochim. Acta* **1978**, 42, 547.
- (24) Hsi, C.-K. D.; Langmuir, D. *Geochim. Cosmochim. Acta* **1985**, 49, 1931.
- (25) Ho, C. H.; Miller, N. H. *J. Colloid Interface Sci.* **1986**, 110, 165.
- (26) Koss, V. *Radiochim. Acta* **1988**, 44/5, 403.
- (27) Hakanen, M.; Lindberg, A. *Sorption of Uranium on Rocks in Anaerobic Groundwater*; Report JYT-92-25; Nuclear Waste Commission of Finnish Power Companies: Helsinki, Finland, 1992.
- (28) Silva, R. J.; Nitsche, H. *Radiochim. Acta* **1995**, 70/71, 377.

Received for review April 29, 1997. Revised manuscript received October 20, 1997. Accepted March 10, 1998.

ES970385U